OPTICAL SIMULATION OF SCRATCH REPAIR IN F/A-18 TRANSPARENCIES

Matti Okkonen[1], Aki Mäyrä[1], Aslak Siljander[2] and Mika Siitonen[3]

[1]VTT Technical Research Centre of Finland Ltd (VTT),
[1]Kaitoväylä 1, FI-90570 Oulu, Finland
[2]Kivimiehentie 3, FI-02150 Espoo, Finland
[3]Finnish Defence Forces Logistics Command,
Vuoreksenkatu 20, FI-33541 Tampere, Finland

Abstract: An on-aircraft system for assessing scratches and dents in F/A-18 transparencies (windshield and canopy) and applying optical simulation for optimizing their repair is presented. The motivation was to automatize the detection and quantification on transparency defects and to assist the manual repair process to minimize induced optical distortions by replacing visual inspection and subjective decision making with automatic, repeatable and objective solution. The information can be applied to optimize the whole logistics chain of the repair process and to maximize aircraft availability. The system developed consist of three consecutive measurement tasks: First a machine vision-based scratch/dent detection and mapping is applied, enabling detecting and classifying defects for further inspection. As a second step, the dimensions of the chosen defects are measured. Thirdly, based on the defect location and dimension, optical simulation is applied to estimate the effect of the repair process, and a most suitable one is chosen regarding optical distortion. The above on-aircraft machine vision system developed for defect detection automatically scans and subsequently maps all defects on the transparencies and provides estimates of their scattering from the pilot's visual perspective. The resulting map enables automatic classification of the scratches and dents found, based on user requirements. It also enables monitoring of the transparency defects' evolution through time, thus providing a modern tool for the transparencies' life cycle management. In addition to the above, an automized optical micrometre was developed for measuring the depth of the scratch or dent, based on 3D imaging. Finally, optical simulation models were developed for connecting the optical distortion induced by the material extraction in the repair process and vice versa. With the simulation, the effect of the repair can be mapped into standardized optical distortion measurement for evaluation. The performance of the defect mapping and depth estimation was assessed by real transparent samples and reference measurements. The simulation models were validated by comparing them with a real defect repair with before and after measurement of optical distortion. The developed system will be fielded to operational use within the Finnish Air Force.

Keywords: optical simulation, aircraft transparencies, transparency repair, automatic defect detection

AUTOMATED TRANSPARENCY DEFECT MAPPING

The first step in the repair process is to locate the defect(s) in the transparency. For this reason, a machine vision-based system was developed to automatically detect and locate light scattering defects on F/A-18C windshield and canopy. As an example of existing methods, some ASTM-standards exists for optical distortion for aircraft windshields [1,2]. The developed system differs from the referenced methods by being a fully automated on-aircraft system; it does not require a dedicated environment for the measurement nor the removal of the transparencies for the inspection. In addition, the developed system can map the defects on both the windshield and canopy that are within the pilot view, and it provides digital maps of their locations including estimates of the visual severity from the pilot viewpoint.

The new method is based on imaging the transparencies from the view of the pilot sitting in the cockpit, while being illuminated from the opposite side of the transparency. The illumination geometry applies a so-called dark field illumination principle, used e.g. in microscopy. The main idea is to enhance the contrast of the scattering defects by providing an illumination geometry where light reaches the camera sensor only when its direction is changed by a defect. Transparency defects, such as scratches and dents, tend to more scatter the light than absorb it, and are thus not easily seen in against an evenly illuminated background. Figure 1 gives a simplified illustration of the dark field illumination principle in this case.

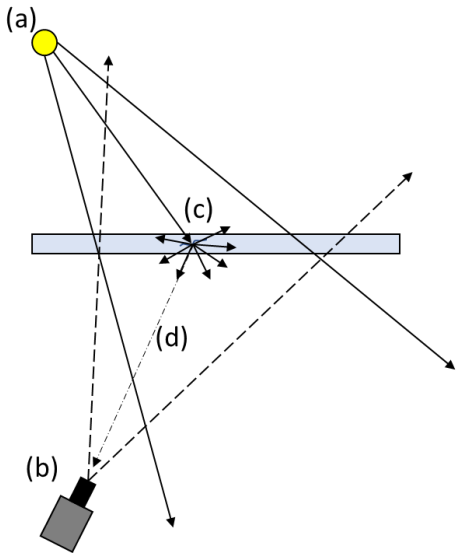

Figure 1. Illustration of the dark field illumination principle as it is applied in the developed system: (a) Light source illuminates the transparency and (b) camera images it from opposite side. A defect (c) scatters the light to multiple direction, and the camera sensor captures only the light that is redirected towards it (d). As the camera does not acquire light from the background, the defect is seen with high contrast.

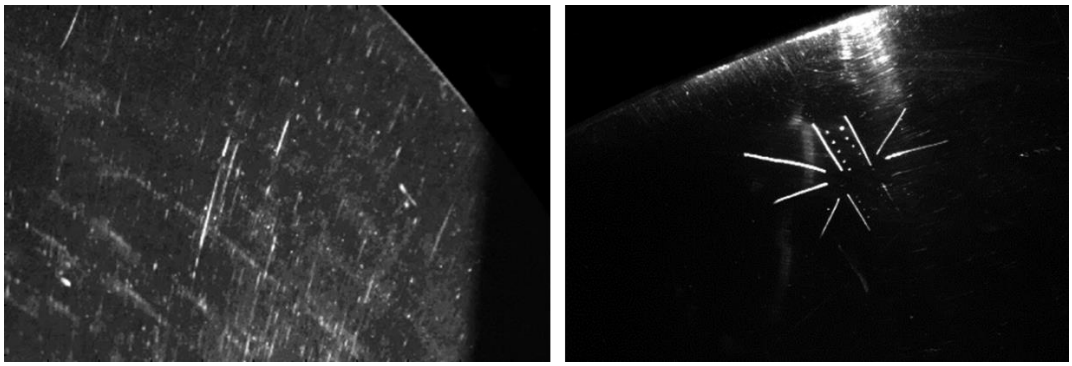

Figure 2. Examples of dark field illuminated transparencies and defects. Left image displays normal wear and tear, whereas right image contains manually made reference defects.

Figure 2. provides examples how dark field illumination highlights scattering defects. Multiple implementations of the dark field illumination were tested in laboratory in order the optimize the contrast of the defects. Specifically, the geometry was set to distinguish between the actual defects, such as scratches and dents, and the background scattering induced by other lower-level wear and tear that exists at some level in all transparencies that are in use. An example of the latter can be seen in the left image in Figure 2. As a result, a spotlight type of a light source was chosen for the task, which illuminates a small area in the transparency and produces good contrast of the defect with minimum amount of ambient light, which can produce reflection and reduce the contrast. In order to map the pilot view of the transparencies in full, multiple light sources are needed to cover the area. This was accomplished by arranging an array of led spotlights on an arc having a constant distance to the windshield surface and which can be shifted along the length of the windshield. Figure 3. illustrates the implementation. The arc is shifted with a fixed step, and in each position the led spots are turned on individually one at a time.

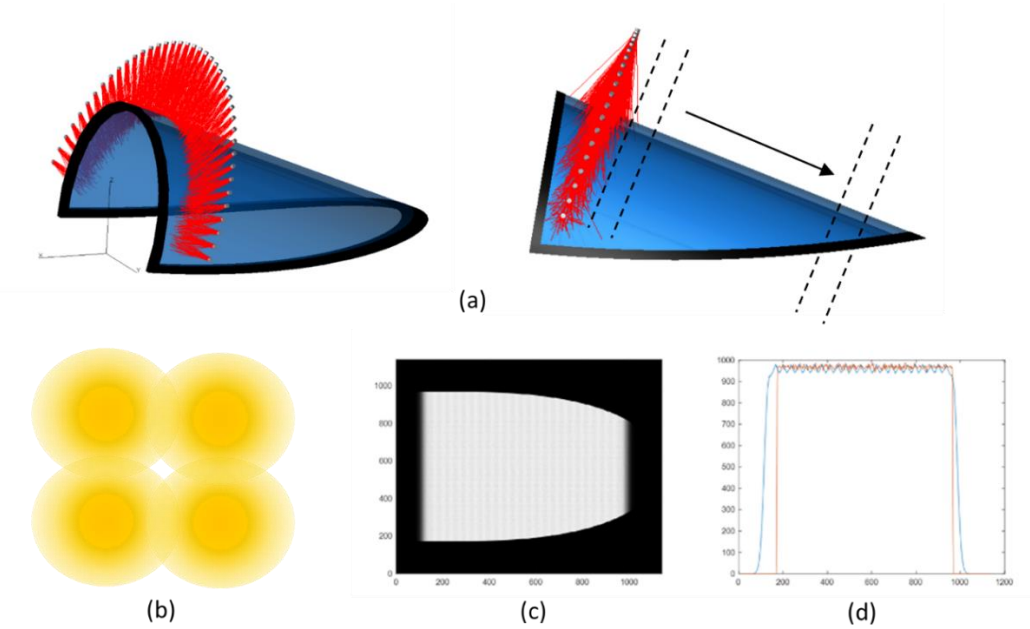

Figure 3. (a) Optical simulation model of the led spotlights arranged as an arch. The arc can be moved along the length of the windshield to cover it in full. (b) The step size of the arc movement and the distance of the leds in the arc are optimized to evenly illuminate the windshield surface. Images (c) and (d) show the combined intensity of the leds on the windshield surface as an image and as a lengthwise profile.

The mechanical implementation of the full on-aircraft system is illustrated in Figure 4. The system scans the windshield and the parts of the canopy visible to pilot. As a result, the system provides an image of both, where the image values are estimates of the amount of light scattering of the transparencies at each point. From the scattering map, defects can be automatically detected and classified according to user needs.

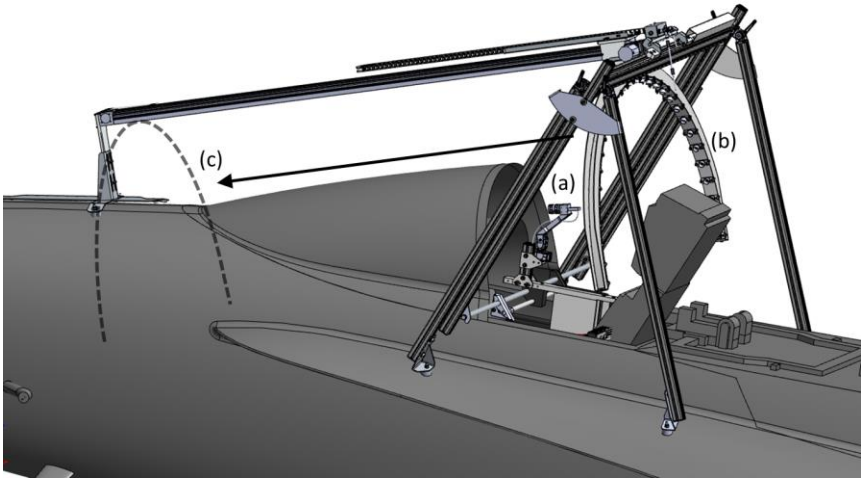

Figure 4. On-plane implementation of the transparency defect mapping system. Main components consist of the camera (a), and the illumination arc (b). (c) The arc moves across length of the windshield to provide dark field illumination to all area that is in pilot view.

HANDHELD SYSTEM FROM DEFECT DIMENSION MEASUREMENT

The above defect mapping system can detect and locate the scattering defects on the transparencies, but more detailed information about the defect dimensions, especially its depth, is needed for the optical simulations. Probably most used method and tool for defect depth measurement in aircraft transparencies is an optical micrometer. It takes advantage of the very limited depth-of-field in microscopic optics, where only the parts of the image that are within a certain depth range appear sharp in the image. Where it is a nuisance in microscopic imaging, here it provides a way to estimate the distance of image areas according to image sharpness. When accompanied with a micrometer, the distance of two object or areas in the image be estimated by adjusting the focal plane manually between them. The disadvantage of such method comes from the manual and visual procedure, where the user must look through the microscope optics and estimate visually when the measured parts of the image are sharp. This involves subjective decisions that can affect the result and can be also very tricky to apply on a transparency which is attached to aircraft.

To overcome these difficulties, a handheld instrument that automates the above process, was developed. It consists of the following main components: industrial digital camera, microscopy optics, a motor and a microcontroller. The measurement procedure follows that of a person using a traditional optical micrometer. Figure 5. illustrates the principle, giving an example of a real scratch measurement. The device is located on a defect (using the location map obtained from the above on-aircraft system), and it automatically captures a stack of images with the depth-of-field having different depths of even intervals, arranged so that the sharp region in the first image is above the transparent surface, and the sharp region in the last one is below the defect bottom. Looking through the stack of images depth-wise, the images where each area is most sharp is estimated. As the depth of the sharp areas of each image is precisely known, the image location in the image stack can be transformed into micrometers, yielding a 3D point cloud of the defect. From there, surface and bottom of the defect can be estimated.

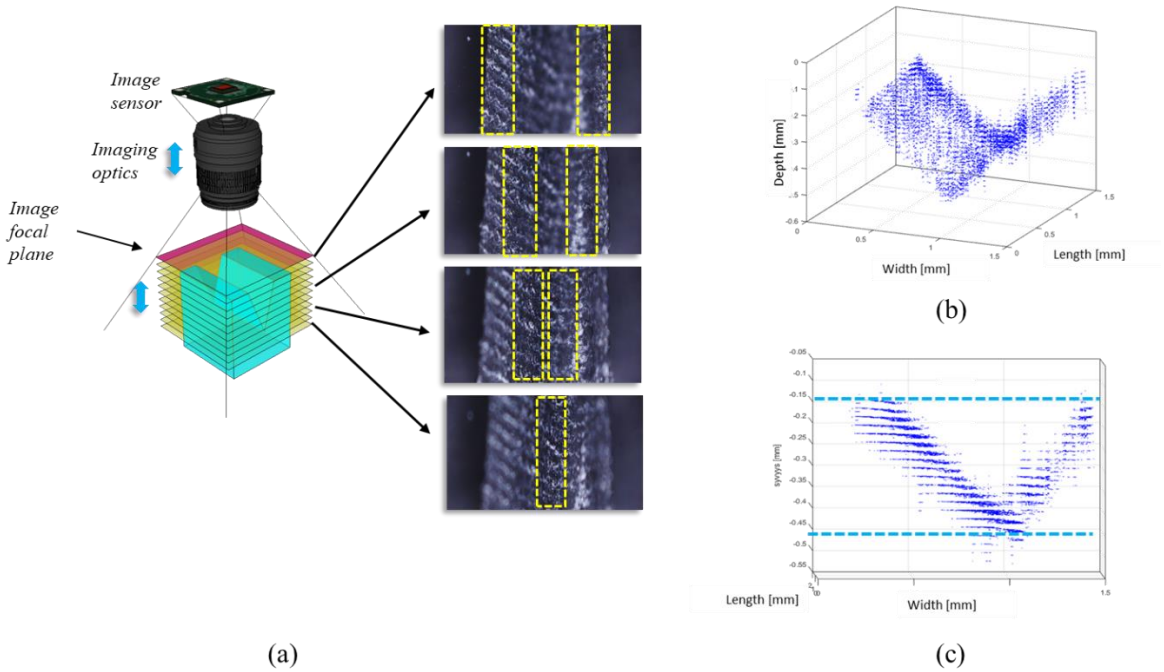

Figure 5. Illustration of the scratch depth estimation principle. (a) Images are captured of the defect with even intervals in depth-wise. Image focal planes illustrate the depth where objects are sharpest in the image. Example images are given, overlayed with areas where the defect appears sharp in the images. (b) The sharpest image in the stack for each pixel position is estimated. As the focal plane depth is known precisely, this provides a depth estimate for each pixel, illustrated as a 3D point cloud here. (c) Finally, the depth of the defect is computed by estimating the top and the bottom (dashed line) of the defect. The image focal plane locations depth-wise are visible in from this angle.

A fully functional handheld user-friendly prototype was developed, illustrated in Figure 6. It encloses the main components, as well as buttons and a color display as a user interface. To verify the principle, a reference sample was made of polycarbonate, having 9 scratches with different depths, ranging from less than 10µm to above 300µm. Reference measurements were made with a white light interferometer (Veeco Wyko NT3300) and with stylus-based profiler (Veeco Dektak 150). In addition, the depths were estimated using a traditional optical micrometer. Figure 7. plots the reference measurement along with the results achieved with the developed depth-of-field based method. For most scratches, the measurements differ only a minor way, which can partly be explained by small differences in the location where the depths were measured. For very small scratches, the developed method has an offset compared to reference method.

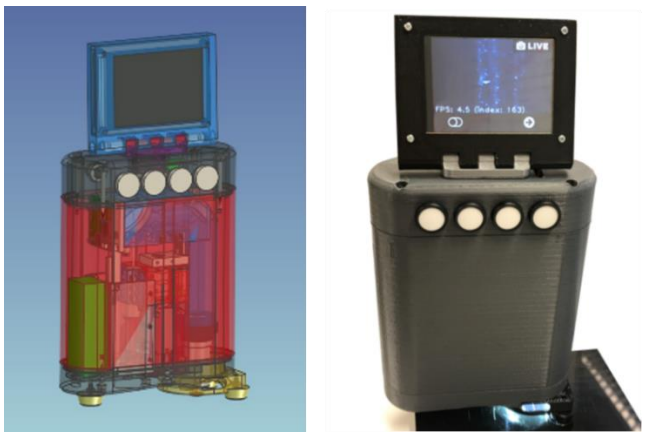

Figure 6. The handheld user-friendly prototype developed for automatic measuring of scratch and dent depth and dimensions.

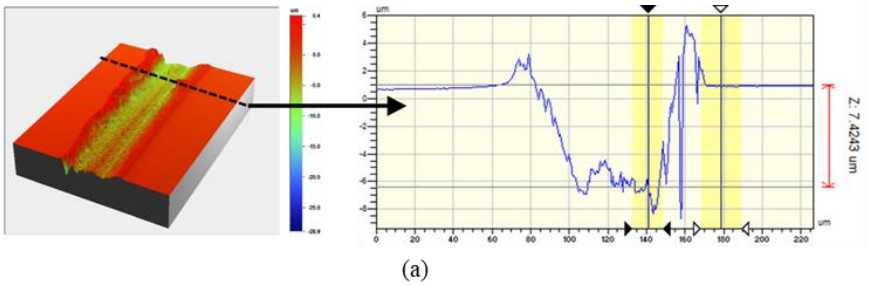

(a)

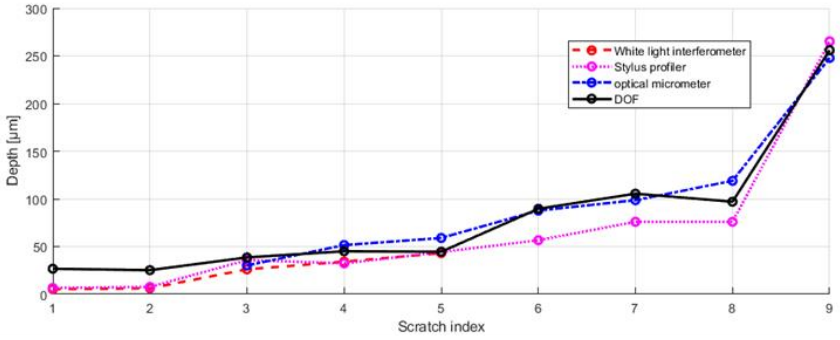

(b)

Figure 7. (a) An example of a reference measurement of a scratch using the Veeco Wyko NT3300 white light interferometer. (b) The developed depth-of-field based (DOF) automized measurement compared to reference measurements and traditional optical micrometer.

OPTICAL SIMULATIONS FOR TRANSPARENT REPAIR

Local curvature deviations or small differences in transparent density or thickness can cause optical distortion. If the distortion is too severe, the operator (pilot) will be disturbed and disoriented during the flight which may lead to expensive transparent rejection or repairs. A good introduction to distortion measurements and decision making can be found in [4] where a machine vision based trained classifier is used to measure and classify in aircraft windshields.

Optical ray tracing can be applied on the transparent repair modelling. The principal idea is to use ray tracing algorithm to evaluate the resulting optical distortion caused by the transparent shape deviations, or vice versa. This reduces subjective biases related to repair related decision making and the following repair efforts. In its simplest form, simulations can be used to evaluate repair induced distortions of a general transparent geometry. In more advanced version, the existing distortions can be modelled on the transparent for which different repairs are proposed and evaluated. In the most advanced version, the transparent repairs can be optimized to meet a pre-defined distortion target.

The main requirements for transparent repair simulations are the optical system description and algorithms related to ray tracing through this system. The system description includes in detail descriptions and locations of the simulated objects, and the algorithm simply calculates the optical refraction and transmissions at each surface. In addition, a computational model which couples the simulated ray tracing results to commonly used distortion standards and measures, like ASTM-standards [1,2], is needed. We have developed a simple system which includes all the required components. Our approach is to model the resulting distortion at the basis of the detected transparent defect, like that of a scratches' or dent's, for which a standard repair pattern is applied, and the resulting distortion is evaluated.

Typical simulation geometry for windshield distortions is shown in Figure 8. The modelled optical layout consists of a transparent, ASTM-style grid board plane and a camera module consisting of a lens objective and a sensor. Ray tracing algorithm is used to trace rays from the sensor to grid board. This allows to model the related distortion ΔX, ΔY caused by the repair related new surface normal N' . In figure, the distorted ray path drawn as dashed line. For simplicity the ray tracing is done from camera end towards the grid board plane. All geometry parameters are adjustable, but selection of ASTM-style geometry will lead to results comparable to common windshield distortion standards. As a result, the distortion from different parts of the transparent can be mapped to grid board images, similarly as in distortion measurements. The bottom left section of Figure 8. shows how evenly sampled transparent points (Figure 9.) map to grid plane. Maximum distortions in horizontal and vertical directions are highlighted on the bottom right of Figure 8.

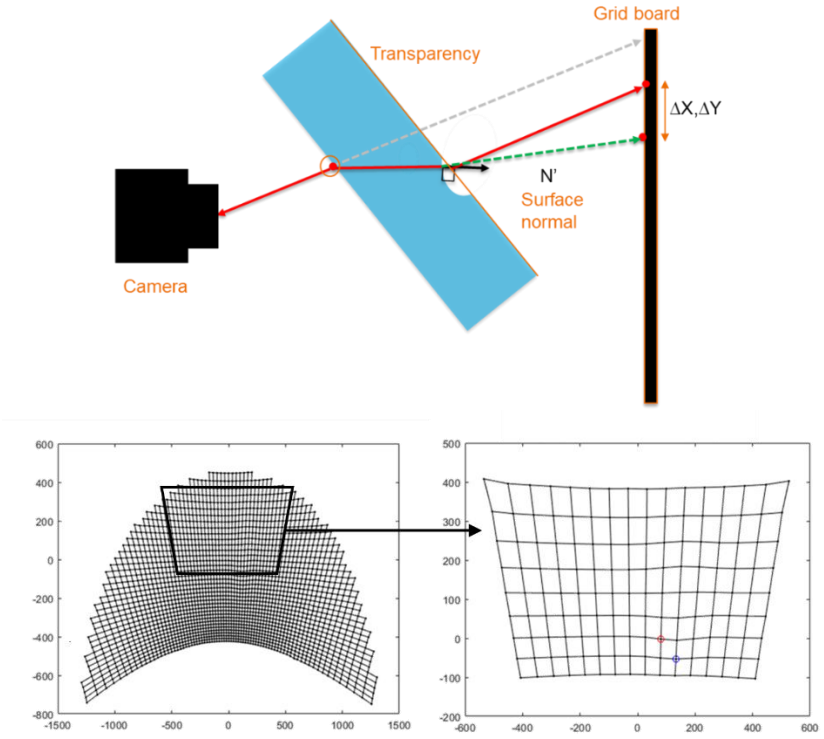

Figure 8. Distortion simulation principle (above) and simulated distortion grid below). Maximum distortions in horizontal and vertical directions are highlighted on the rightmost zoom figure. All axis units are in (mm).

Presented simulations can be further complemented by optimization routines which can either propose pre-selected repair patterns to be modelled or which use pre-defined target criterion for which the repairs are optimized.

Trial with real transparent repair

The performance of the repair simulation algorithm was assessed by real transparent samples and measurements. The trial included a real defect repair with before and after measurement of optical distortion. In our trial, a sample scratch was created on a scrap transparent. This scratch was measured to be roughly 100 µm deep after which the scratch area was manually polished. Scratch location and polished area are shown in Figure 9. (left) and grid imaging in Figure 9. (right).

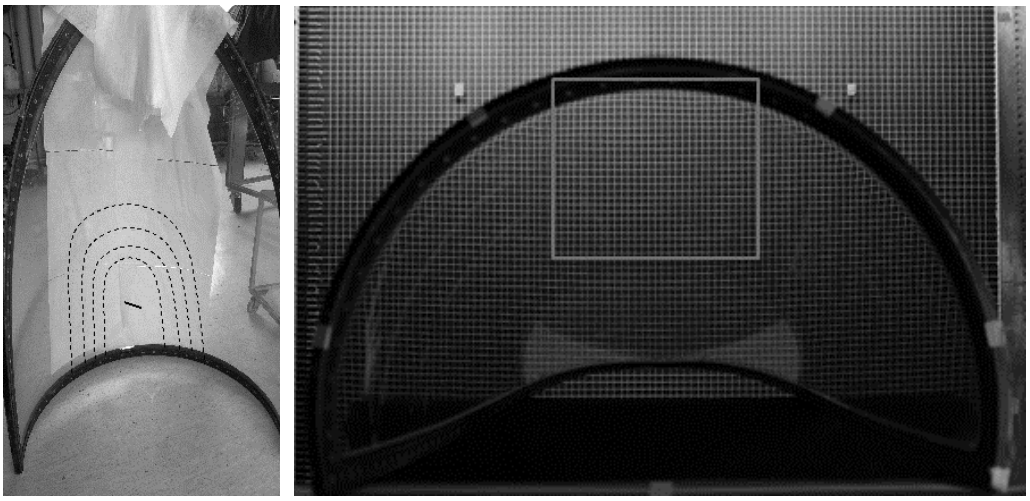

Figure 9. Location of the sample scratch and estimated areas of material removal (left) and sample of the grid image (right). Estimated region of interest is marked on the grid image.

The measured grid image pairs were used to solve spatial normal deviations, *N'* in Figure 8 (above), on the transparent surface in the region of interest (Figure 8. below and Figure 9. right). These normal vectors were locally subtracted, and the resulting gradient field (Figure 10. centre) was integrated to a 3-dimensional surface [8] shown in Figure 10. right. This surface serves as an estimate of the thickness deviation which is caused by the repair process. In the sampled region the estimated valley depth is slightly larger than 100 um which is well in line with the measured scratch depth and the shape of the polished area visualised in Figure 9 left.

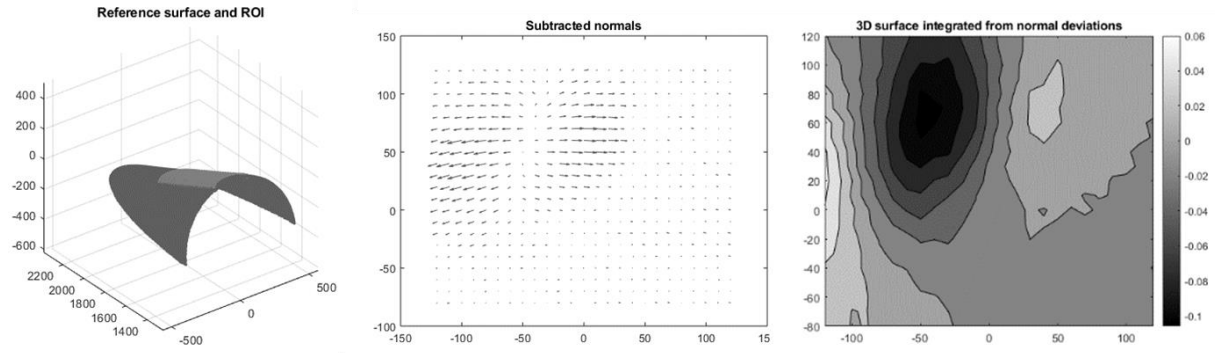

Figure 10. Reference surface profile (left), subtracted normal vectors visualized in 2D (center) and a 3D-surface integrated from the gradient vectors at the transparent coordinates (right). All axis units are in (mm).

SUMMARY

An on-aircraft system for assessing scratches and dents in F/A-18 transparencies and applying optical simulation for optimizing their repair was presented. The system consists of three consecutive phases: First defects are automatically mapped both in windshield and canopy, for which an on-aircraft, machine vision based system was developed. Secondly, a handheld instrument for estimating the detailed dimensions was developed, automatizing the principle of optical micrometer for measuring the defect depth. Finally, optical modelling was used to assess the repair process and finding optimal parameters for it regarding optical distortions. All phases were successfully tested with real samples, and the system is intended to be fielded for operational use in the Finnish Defence Forces.

ACKNOWLEDGMENETS

Patria Aviation is acknowledged for their work and vital support in the repair trials, and for providing related images.

REFERENCES

[1] ASTM international, "Standard Test Method for Measuring Optical Distortion in Transparent Parts Using Grid Line Slope 1," *F 2156 – 01*. 2001.
[2] ASTM international, "Standard Practice for Optical Distortion and Deviation of Transparent Parts Using the Double-Exposure Method 1," *F 733 – 90*. 2003.
[3] Aikens, D. (2017). In: *New options for optical quality tolerances*, Proceedings of SPIE, vol. 10590, p. 105900J.
[4] Dixon, M., *et al.* (2011). *Measuring optical distortion in aircraft transparencies: A fully automated system for quantitative evaluation*, Mach Vis Appl, vol. 22, no. 5, pp. 791–804.
[5] Okkonen, M. and Mäyrä, A. (2018). *Optical Simulation of Scratch Repair in FA-18C*, Workshop on Transparent Enclosures and Materials, F07 Aerospace and Aircraft, ASTM.
[6] Okkonen, M. and Mäyrä, A. (2017). *XPARENCY – Overview, spinoffs, future activities*, Workshop on Transparent Enclosures and Materials, F07 Aerospace and Aircraft, ASTM.
[7] Okkonen, M. and Mäyrä, A. (2014). *New angles for transparency distortion measurements*, Workshop on Transparent Enclosures and Materials, F07 Aerospace and Aircraft, ASTM.
[8] Harker, M. and O'Leary, P. (2023). *Surface Reconstruction from Gradient Fields: grad2Surf*, MATLAB Central File Exchange, Accessed: Feb. 13, 2023. [Online]